Published in final edited form as:

Nat Catal. 2021 February ; 4(2): 164–171. doi:10.1038/s41929-020-00569-8.

Gold-catalysed asymmetric net addition of unactivated propargylic C–H bonds to tethered aldehydes

Ting Li[†,‡,≠,#], **Xinpeng Cheng**[†,≠], **Pengcheng Qian**[‡,*], **Liming Zhang**[†,*]

[†]Department of Chemistry and Biochemistry, University of California, Santa Barbara, CA 93106, USA

[‡]Key Laboratory of Environmental Functional Materials Technology and Application of Wenzhou City, College of Chemistry & Materials Engineering, Institute of New Materials& Industry Technology, Wenzhou University, Wenzhou 325000, China

Abstract

The asymmetric one-step net addition of unactivated propargylic C-H bond to aldehyde leads to an atom-economic construction of versatile chiral propargylic alcohols but has not been realized previously. Here we show its implementation in an intramolecular manner under mild reaction conditions. Via cooperative gold catalysis enabled by a chiral bifunctional phosphine ligand, this chemistry achieves asymmetric catalytic deprotonation of propargylic C-H ($pK_a > 30$) by a tertiary amine group ($pK_a \sim 10$) of the ligand in the presence of much more acidic aldehydic α-hydrogens (pKa ~ 17). The reaction exhibits a broad scope and readily accommodates various functional groups. The 5-/6-membered ring fused homopropargylic alcohol products are formed with excellent enantiomeric excesses and high *trans*-selectivities with or without a preexisting substrate chiral center. DFT studies of the reaction support the conceived reaction mechanism and the calculated energetics corroborate the observed stereoselectivity and confirm an additional metal-ligand cooperation.

Graphical Abstract

[*]Corresponding authors: zhang@chem.ucsb.edu, qpc@wzu.edu.cn.

[#]Current address: College of Chemistry and Pharmaceutical Engineering, Nanyang Normal University, Nanyang, Henan 473061, P. R. China

[≠]These authors contributed equally.

AUTHOR CONTRIBUTIONS

TL conducted the experiments and prepared a draft of the manuscript. XC synthesized the ligands and their gold catalysts and helped with the manuscript. PQ secured TL's postdoctoral fellowship from Wenzhou University and participated in the chemistry design. LZ designed the chemistry and supervised its implementation and finalized the manuscript.

COMPETING INTERESTS

The authors declare no competing interests.

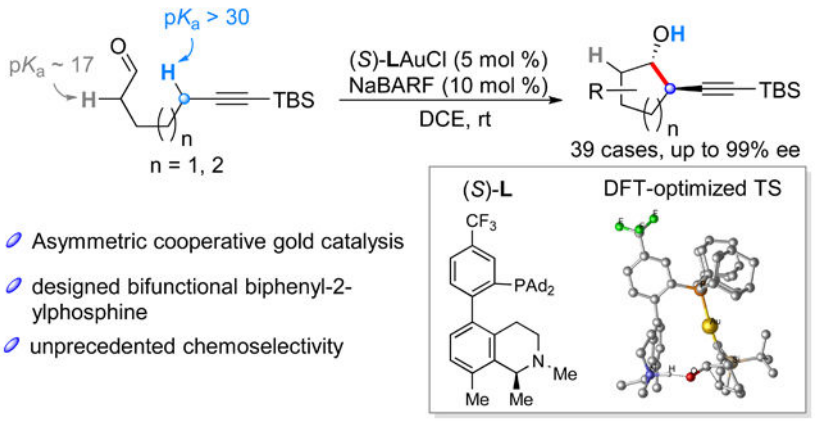

INTRODUCTION:

Asymmetric propargylation of aldehyde leads to versatile chiral homopropargylic alcohol products and is of exceptional importance in organic synthesis.[1,2] In these reactions, in order to achieve asymmetry, allenylmetal species featuring Si, B, Al, Cu, Sn, Cr, In and etc. serve as the propargylic nucleophile and are either prior prepared or generated in situ via transmetallation with a propargylmetal precursor or from propargylic halides in the presence of reducing metal (Figure 1A). This requirement of prefunctionalization at the propargylic position or the allene is conceptually much less appealing than the direct asymmetric net addition of a propargylic C-H bond to a carbonyl group. The latter process is completely atom economic, avoids the use of stoichiometric metal and/or costly substrates and the generation of stoichiometric metal salt waste, and could be achieved via sequential deprotonation-propargylation-protonation in a catalytic manifold. This type of chemistry constitutes a catalytic asymmetric propargylic C-H functionalization[3–11] but to be the best of our knowledge has no literature precedent. In the recently-reported racemic case,[11] aldehyde substrates possessing α-C(sp^3)-H bonds are not permitted. Such substrates are challenging and appear not conceptually feasible under typical basic conditions as the propargylic protons are much less acidic (*p*Ka >30) than aldehyde α-hydrogens (*p*Ka ~17) in an ionic reaction manifold (Figure 1B). Instead, self-aldol reaction/condensation would be the dominant reaction pathway.

In an earlier report by our lab,[12] we realized a net addition of a propargylic C-H bond to an aldehyde in a propargylation reaction under homogeneous Au(I) catalysis. As shown in Figure 1C, in the presence of a gold(I) catalyst containing an achiral biphenyl-2-ylphosphine ligand **L1** featuring a remote tertiary amino group,[13–17] the intermolecular propargylation of aldehyde by a silylated alkyne occurs smoothly, and the propargylic alcohol **1** generated undergoes further silyl-migrative cyclization to deliver the dihydrofuran product **2**.[18] Mechanistic studies confirmed the intermediacy of **1**. The reaction is proposed to proceed via a σ-allenylgold intermediate (i.e., **A**), the generation of which entails the extraordinary deprotonation of the propargylic C-H bond (pKa>30) by the tertiary amino group (pKa ~ 10) and is enabled by the cooperative activation of the C-C triple bond by the appropriately positioned Lewis acidic gold(I) center. Besides being racemic, this

reaction suffers severe scope limitations: the propargylic C-H bond needs to be activated by an aryl/alkenyl substituent and the aldehyde needs to be activated by an electron-deficient unsaturated group and cannot accommodate any α-C(sp^3)-H bonds.

In this work, we report the asymmetric intramolecular net addition of unactivated propargylic C-H bond to aldehydes in a catalytic manner. By developing a chiral bifunctional ligand, the reactions exhibit mostly excellent enantioselectivities and diastereoselectivities and tolerate aldehydes possessing α-C(sp^3)-H bonds. Of great significance is the chemoselective deprotonation, the ready accommodation of a substrate preexisting chiral center of either configuration and the high synthetic value of the cyclic products.

Results

Reaction discovery and optimization.

At the outset, we chose the TBS (*tert*-butyldimethylsilyl)-terminated hept-6-ynal (**3a**) as the substrate for reaction discovery and optimization. It is anticipated that chemoselective deprotonation of its propargylic H_a over the aldehydic H_b in the presence of a cationic gold(I) ligated by our recently developed bifunctional phosphine ligand, despite the latter being more acidic, is plausible due to the above-discussed cooperative deprotonation of propargylic C-H bonds by the mild basic ligand tertiary amine. Such a process would generate a nucleophilic σ-allenylgold intermediate and hence permit cyclization to form the *trans*-ring-fused homopropargylic alcohol **4a** and its *cis*-isomer in a catalytic setting. Much to our delight, with achiral **L1** as the ligand and the reaction temperature at 60 ˚C, **4a** was indeed formed as the major product along with **4a'**, **4a''** and **4a'''** (entry 1). It should be noted that the *cis*-**4a** was not detected from the reaction mixture. It appears that **4a'**, **4a''** and **4a'''** were generated from *cis*-**4a** as **4a** could not be converted to these side products under identical reaction conditions. Not to our surprise, JohnPhos, a biphenylphosphine ligand similar to **L1** with regard to electronics and sterics but lacking the remote amino group, led to no reaction at all, and the addition of Et_3N did not help, either (entries 2 and 3). These results again highlight the critical role of the cooperating amino group in the gold catalysis.

With this encouraging result in hand, we turned our attention to asymmetric catalysis. We previously developed the ligand (*R*)-**L2**, a chiral version of **L1**, for the asymmetric isomerization of alkynes to chiral allenes *en route* to chiral dihydrofuran products.[19] The general design considerations leading to the chiral ligand are shown in Table 1, that is, the R group at the ligand chiral center can shield the basic nitrogen from participating in the reaction in one of the two biaryl axis configurations, and consequently the ligand center chirality can be employed to achieve the desired ligand axis chirality for asymmetric gold catalysis. Coupled with the fluxional nature of the axis, both atropisomers of the catalyst may effectively participate in catalysis. In that reaction, a chiral σ-allenylgold intermediate of type **A** (see Fig. 1C) is generated en route to a chiral allene intermediate. It is reasoned that with (*R*)-**L2** as the ligand this intramolecular propargylation could become enantioselective. Much to our delight, with (*R*)-**L2**Au^+ as the catalyst, the cyclization

delivers **4a** in 55% yield in −93% *ee* (its configurations are opposite to those in the shown structure, entry 4).

To improve this reaction, we undertook further ligand optimization. Our DFT calculations of the tetrahydroisoquinoline portion of **L2** at M06–2x/cc-pVDZ level revealed that the nitrogen-exposed conformer **B** is 3.605 kcal/mol less stable than the nitrogen-buried conformer **B'** due to the gauche interaction between *N*-Me and the cyclohexyl group. As such, the desired conformer **B** is a minor component. To make the exposed conformer energetically less disfavored, we reason that minimizing the Cy group into a Me group would decrease the destabilizing gauche interaction. To maintain a pseudo-axial orientation of the Me group, a 8-methyl group should be installed in order to enhance the $A^{1,3}$-strain when it is pseudo equatorially oriented. Indeed, DFT calculations confirmed that the two conformations of 1,8,*N*-trimethyltetrahydroquinoline, i.e., **C** and **C'**, are energetically nearly equal. To this end, the corresponding ligand (*S*)-**L3** was prepared[20] and its structure was confirmed by X-ray diffraction studies of its AuCl complex (Figure 2a). To our delight, it led to a better yield of **4a** (77%) and an excellent ee (99%, entry 5). **4a'**, **4a''** and **4a'''** were barely detected, indicating a *trans*/*cis* selectivity of >13 in the cyclization step. The absolute configuration of **4a** was assigned based on the X-ray diffraction study of one of its homologs (see Figure 2b, *vide infra*). The counter anion of the in-situ generated cationic gold(I) catalyst is also of critical importance, and only $BARF^-${tetrakis[3,5-bis(trifluoromethyl)-phenyl]borate} worked well. The use of other commonly employed anions such as OTf^- (entry 6) and NTf_2^- (entry 7) resulted in no products at all. When $Ag(CH_3CN)_2^+$ $BARF^-$ was used instead of $NaBArF_4$, the reaction yield was 40% (entry 8). In addition, the solvent DCE is important for the optimal yield as $PhCF_3$ and THF led to lower yields (entries 9−10).

Reaction scope studies.

With the optimized reaction conditions in hand, we set out to investigate the reaction scope. First, silyl protecting groups other than TBS were examined. As shown in Table 2, the much smaller TMS group led to no target product 4b, and only the aldehyde oxidation product 7-(trimethylsilyl)hept-6-ynoic acid was detected. Furthermore, running the reaction under argon did not permit the desired reaction, either. However, other bulkier silyl groups including $SiMe_2Ph$ (4c), $SiMePh_2$ (4d), and TBDPS (4e) were allowed, and TBDPS led to an excellent yield but a slightly lower ee. Further studies revealed that the installment of a fused benzene ring in the substrate backbone was allowed, and products 4f and 4g were obtained in moderate yields and with excellent enantioselectivities. Switching the chiral ligand to its enantiomer led to essentially identical results with the opposite product stereochemistry. Substrates containing oxygen at different positions of the backbone such as 3h, 3i, and 3j all underwent the reaction smoothly, affording the tetrahydrofuran or dihydrofuran products with excellent *ee* value. The dihydrobenzofuranol 11, prepared upon desilylation of 4j, was subjected to X-ray diffraction studies. As shown in Figure 2b, it exhibits the (1*R*, 2*R*)-configuration. Consequently, the configurations of the nascent chiral centers of all the five-membered ring products were assigned accordingly. Substituents of varying electronic and steric characteristics are generally allowed in this transformation, leading to products 4k–4x in good yields and excellent enantioselectivities. It should be noted that some of them, i.e., 4k–4m and 4r–4x, possess an additional stereocenter and

were synthesized from the corresponding racemic substrates. The exceptional levels of asymmetric induction (mostly ≥98% ee) with either substrate enantiomer highlight the extraordinary catalyst-dictated asymmetric induction independent of substrate chirality, a highly valuable feature in asymmetric catalysis that permits flexible and selective access to different product stereoisomers by simply varying substrate and catalyst chirality. Some of the diastereomeric products, i.e., 4k-4m, 4r, 4t, 4u, and 4w, are separable and were individually characterized. In all the cases except 4m, the configurations of the stereogenic centers inherited from substrates were assigned based on the splitting pattern of the middle carbon proton of the stereochemical triad, where a triplet with $^{3}J_{\text{H-H}}$ ranging from 5 to 9 Hz in one stereoisomer is assigned with the *trans-trans* arrangement while its epimer displays a doublet of doublet or a pseudo triplet with $^{3}J_{\text{H-H}}$ around 2–3 Hz and hence is assigned with the *trans-cis* arrangement. These assignments are further supported in some cases by observed NOE (nuclear overhauser effect) and by related literature observations.[21–23] The stereochemistry of 4m was tentatively assigned by assuming that in the *1S*, 2*R*, 4*S*-isomer its alkynyl group is in the bisected position and the HO and TBDPSO (*tert*-butyldiphenylsiloxy) groups are in equatorial positions in an envelope conformer. Notably, substrates bearing the severe steric hindrance such as 4n and 4o and the spiro substrates 4p and 4q all worked well in this chemistry, indicating the steric hindrance around the aldehyde group is inconsequential. Replacing the phenyl group of 4r with other heterocycles including 2-naphthyl (4u), 3-indolyl (4v), and 3-thienyl (4w) were also successful. To expand the scope, we also examined the alkyl group in place of the 4r aryl group, and the desired product 4x was smoothly formed.

It is worth noting that we could not find any literature asymmetric chemical synthesis of desilylated **4a**, the simplest structure in the reaction scope, by Scifinder despite its commercial availability. The stereochemically more complex **4k**-**4m** and **4r**-**4x** present additional synthetic challenges, especially considering the issues associated with regioselectivity in the synthetic approach of epoxide ring-opening (e.g., **4k** and **4l**[24]**)** and the inevitable shortcomings of stereochemical inflexibility due to substrate stereocontrol. This chemistry, on the other hand, provides a general, highly stereoselective and stereo-flexible strategy to access these synthetically valuable cyclopentanols.

We then turned our attention to the asymmetric construction of 6-membered ring-fused homopropargylic alcohols. The brief reaction optimization is shown in Table 3. Initially, no desired product **6a** was formed under the conditions optimized for the cyclopentanol formation (entry 1). However, it was later found that when the reaction was performed under argon and with 20 mol% $NaBARF_4$ the reaction of **5a** delivered the desired product *cis*-**6a** in 70% yield and with 98% *ee*. The opposite high enantioselectivity was realized with (*R*)-**L3** as the ligand (entry 4). However, (*R*)-**L2** is a markedly inferior ligand for the asymmetric induction, resulting in only −76% ee (entry 3).

The reaction scope was then investigated. As shown in Table 4, benzene fusions at the substrate backbone were allowed, and the anticipated *trans*-homopropargylic alcohol products **6b**, **6c**, and **6d** were obtained in serviceable yields and with excellent enantioselectivities. An oxygen-based substituent, being an oxo (**6e**), a siloxyl (**6f** or **6g**) or a BnO (**6h**) were tolerated, and the reactions again exhibited excellent asymmetric induction,

regardless of the preexisting stereochemistry in the case of **6f**-**6h**. In the case of **6f**, the relatively high ratio of the diastereomeric products reveals that the substrate (*S*)-enantiomer exhibits substantially higher reactivity than its (*R*)-enantiomer. This is unusual as in most cases substrate enantiomers exhibit similar reactivities. Substrates containing oxygen in the linker between the reacting functional groups were also tested, and the *trans*-tetrahydropyran products **6i**, **6j**, and **6k** were formed with excellent enantioselectivities. In the cases of **6i** and **6k**, the corresponding *cis*-isomers were also detected as the minor product and interestingly with markedly lower ee. Of note, **6i** was characterized as the separable benzoates. A phenyl substitution at the homopropargylic position of **6j** in the case of **6l** was readily permitted, and the substrate chirality again had little impact on the ligand-imposed asymmetric induction, affording both epimers of the trisubstituted tetrahydropyran **6l** in a combined yield of 88% and with excellent ee. Moreover, different substitutions on the phenyl ring including *o*-F (**6m**), *m*-MeO (**6n**) and *p*-CF_3 (**6o**) or its replacement with a 2-thiophenyl (**6p**) were readily accommodated, and the tetrahydropyran products were isolated in good yields and with ee values ranging from 92% to 98%. Although **6p** was isolated as a chromatographically inseparable viscous liquid at room temperature, upon storing at −20 ˚C in a freezer, one isomer crystallized out, and its X-ray diffraction studies established the configurations of its newly generated stereocenters as *3R*, 4*S*, which are identical to those in the five-membered ring products (Fig. 2c). Consequently, the configurations of these stereocenters in all the other products **6** were assigned accordingly. The configurations of the inherited chiral centers in **6f**-**6h** and **6l**-**6o** were assigned based on ^{1}H-^{1}H coupling patterns.

Similarly, to the best of our knowledge, there is no reported synthetic method for the desilylated (1*S*, 2*R*)-**6a** and a general lack of highly stereoselective access to the cyclohexanols shown in Table 4. Considering the ubiquity of these ring systems, this chemistry avails them for various synthetic applications.

DFT calculation.

To offer insights into the reaction mechanism and to understand the observed stereoselectivities, we performed DFT studies of the reaction of **3a.** As shown in Figure 3, the deprotonation transition state **TS-allene-2** leading to the allenylgold intermediate **E** with an (*aR*)-allene is favored by 4.0 kcal/mol over **TS-allene-1**, which leads to the opposite allene configuration. This difference in activation energy can be largely attributed to the indicated steric congestion in the latter and consistent with the observed high enantioselectivities. The deprotonation follows a syn-periplanar process[25] with the dihedral angle of Au-C1-C3-H being 11.2° in **TS-allene-1** and 26.7° in **TS-allene-2**. Subsequent cyclizations of the kinetically favored allenylgold **E** only need to overcome barriers of 3.8 kcal/mol and 2.1 kcal/mol to form the gold-coordinated cyclopentanols ***cis*-4a-Au** and ***trans*-4a-Au**, respectively. These barriers are much lower than 6.4 kcal/mol needed for **E** to revert back to **D**, suggesting that the equilibrium between **E** and its allene epimer via **D** is not operative. The *trans*-cyclization leading to ***trans*-4a-Au** is favored by 1.7 kcal/mol with regard to the reaction barrier over the competing *cis*-cyclization, despite there is little difference in product stability. This is consistent with the observed formation of **4a** as the major product. Moreover, in both the transition states **TS-cy-cis** and **TS-cy-trans**, the distances between the ligand ammonium proton and the aldehyde oxygen are 1.395 Å and

1.386 Å, respectively, indicating the activation of aldehyde by the acidic ligand proton and confirming additional cooperation between metal and ligand in the chemistry. Finally, the configurations of the cyclopentanol moiety in ***trans*-4a-Au** are identical to our experimental assignments.

Synthetic applications.

The presence of a hydroxyl group provided a versatile handle for the functionalization of the products. As shown in Figure 4, the products *trans*-**4a** or *trans*-**6a** could be easily transformed to cis-**7a**, cis-**8a** and cis-**9a** in excellent yields and enantiopurities via the Mitsunobu reaction. These results established that all four stereoisomers of the fused homopropargylic alcohols can be accessed with high to excellent stereoselectivity via this gold catalysis, which is of significant synthetic value. The products could also be easily transformed into the 1,7-enynes derivative **10**, which can undergo cyclization to provide enantiomerically enriched cyclohexane derivatives containing the boron and silicon functional groups by following a racemic literature precedent.[26] Similarly, the functionalized dihydrofuran-3-one could be accessed starting from **10** following another literature report.[27]

Conclusions

We have achieved catalytic asymmetric net addition of unactivated propargylic C-H bond to tethered aldehyde. Employing a ligand-enabled cooperative gold catalysis, this reaction achieves selective deprotonation of propargylic C-H (p*K*a > 30) by a rather weak tertiary amino group (p*K*a ~ 10) in the presence of substantially more acidic aldehydic α-hydrogens (p*K*a ~ 17). Aldehydes possessing α-C(sp^3)-H, not permitted in two precedents, are readily tolerated by this reaction, and the 5-/6-membered ring fused products are generated with excellent enantiomeric excesses and diastereoselectivities. For substrates possessing a chiral center in either configuration, this asymmetric gold catalysis maintains exceptional levels of asymmetric induction, affording ring-fused homopropargylic alcohol products with increasing stereochemical complexity. These chiral cyclopentanols and cyclohexanols are of exceptional synthetic values, yet the preparation of these products is synthetically challenging. This chemistry provides a facile access to them. Our DFT studies support the conceived mechanism, corroborate the stereochemical assignments and the observed stereoselectivity, and confirm ligand-metal cooperation in the cyclization step. This propargylic C-H functionalization strategy opens a highly valuable venue to further asymmetrically transform unactivated alkynes α-C-H bonds under mild catalytic conditions.

Methods

General synthetic procedure for chiral homopropargylic alcohol 4

A 3-dram vial with a magnetic stir bas was charged with aldehyde **3** (0.2 mmol), NaBARF (0.02 mmol, 17.7 mg, 10 mol %), **L3**AuCl (0.01 mmol, 8.5 mg, 5 mol %), and dry DCE (0.4 mL). The vial was sealed with a cap and stirred at room temperature. Reaction progress was monitored by TLC. Upon completion, the reaction was concentrated under reduced pressure. The residue was purified by silica gel flash column chromatography to obtain the desired product.

Data availability

Experimental procedures, characterization of compounds and DFT calculation are available in the Supplementary Information. The X-ray diffraction data for **11**, **6p**, and (*S*)-**L3**AuCl are deposited to the Cambridge Crystallographic Data Centre (CCDC) with the reference numbers 1988012, 1988013, and 1988482, respectively. All data are available from the authors upon reasonable request.

Supplementary Material

Refer to Web version on PubMed Central for supplementary material.

ACKNOWLEDGMENTS

LZ thank NIH R01GM123342 and NSF CHE 1800525 for financial support and NSF MRI-1920299 for the acquisition of Bruker 500 MHz and 400 MHz NMR instruments. The DFT studies were performed using the computational facilities purchased with funds from the National Science Foundation (CNS-1725797) and administered by the Center for Scientific Computing (CSC). The CSC is supported by the California NanoSystems Institute and the Materials Research Science and Engineering Center (MRSEC; NSF DMR 1720256) at UC Santa Barbara.

References

1. Ding C-H & Hou X-L Catalytic asymmetric propargylation. Chem. Rev 111, 1914–1937 (2011). [PubMed: 21344874]
2. Yang X, Kalita SJ, Maheshuni S & Huang Y-Y Recent advances on transition-metal-catalyzed asymmetric tandem reactions with organoboron reagents. Coord. Chem. Rev 392, 35–48 (2019).
3. Alvarez LX, Christ ML & Sorokin AB Selective oxidation of alkenes and alkynes catalyzed by copper complexes. Appl. Catal. A 325, 303–308 (2007).
4. Cheng D & Bao W. Propargylation of 1,3-dicarbonyl compounds with 1,3-diarylpropynes via oxidative cross-coupling between sp^3 C−H and sp^3 C−H. J. Org. Chem 73, 6881–6883 (2008). [PubMed: 18656984]
5. Grigg RD, Rigoli JW, Pearce SD & Schomaker JM Synthesis of propargylic and allenic carbamates via the C–H amination of alkynes. Org. Lett 14, 280–283 (2012). [PubMed: 22182178]
6. Wang T, Zhou W, Yin H, Ma J-A & Jiao N. Iron-facilitated oxidative dehydrogenative C-O bond formation by propargylic C-H functionalization. Angew. Chem. Int. Ed 51, 10823–10826 (2012).
7. Lu H, Li C, Jiang H, Lizardi CL & Zhang XP Chemoselective amination of propargylic C(sp3)-H bonds by cobalt(II)-based metalloradical catalysis. Angew. Chem. Int. Ed 53, 7028–7032 (2014).
8. Fernández-Salas JA, Eberhart AJ & Procter DJ Metal-free CH–CH-type cross-coupling of arenes and alkynes directed by a multifunctional sulfoxide group. J. Am. Chem. Soc 138, 790–793 (2016). [PubMed: 26745643]
9. Hu G, Xu J & Li P. Sulfur mediated propargylic C–H alkylation of alkynes. Org. Chem. Front 5, 2167–2170 (2018).
10. Ju M et al. Silver-catalyzed enantioselective propargylic C–H bond amination through rational ligand design. J. Am. Chem. Soc 142, 12930–12936 (2020). [PubMed: 32659081]
11. Wang Y, Zhu J, Durham AC, Lindberg H & Wang Y-M α-C–H functionalization of π-bonds using iron complexes: catalytic hydroxyalkylation of alkynes and alkenes. J. Am. Chem. Soc 141, 19594–19599 (2019). [PubMed: 31791121]
12. Li T & Zhang L. Bifunctional biphenyl-2-ylphosphine ligand enables tandem gold-catalyzed propargylation of aldehyde and unexpected cycloisomerization. J. Am. Chem. Soc 140, 17439–17443 (2018). [PubMed: 30525525]
13. Wang Z, Wang Y & Zhang L. Soft propargylic deprotonation: designed ligand enables Au-catalyzed isomerization of alkynes to 1,3-dienes. J. Am. Chem. Soc 136, 8887–8890 (2014). [PubMed: 24911158]

14. Wang Z, Ying A, Fan Z, Hervieu C & Zhang L. Tertiary amino group in cationic gold catalyst: tethered frustrated lewis pairs that enable ligand-controlled regiodivergent and stereoselective isomerizations of propargylic esters. ACS Catal. 7, 3676–3680 (2017).
15. Li X, Ma X, Wang Z, Liu P-N & Zhang L. Bifunctional phosphine ligand enabled gold-catalyzed alkynamide cycloisomerization: access to electron-rich 2-aminofurans and their Diels–Alder adducts. Angew. Chem., Int. Ed 58, 17180–17184 (2019).
16. Li X, Wang Z, Ma X, Liu P-N & Zhang L. Designed bifunctional phosphine ligand-enabled gold-catalyzed isomerizations of ynamides and allenamides: stereoselective and regioselective formation of 1-amido-1,3-dienes. Org. Lett 19, 5744–5747 (2017). [PubMed: 29035053]
17. Wang H, Li T, Zheng Z & Zhang L. Efficient synthesis of α-allylbutenolides from allyl ynoates via tandem ligand-enabled Au(I) catalysis and the claisen rearrangement. ACS Catal. 9, 10339–10342 (2019).
18. Li T, Yang Y, Li B, Bao X & Zhang L. Gold-catalyzed silyl-migrative cyclization of homopropargylic alcohols enabled by bifunctional biphenyl-2-ylphosphine and DFT studies. Org. Lett 21, 7791–7794 (2019). [PubMed: 31532214]
19. Cheng X, Wang Z, Quintanilla CD & Zhang L. Chiral bifunctional phosphine ligand enabling gold-catalyzed asymmetric isomerization of alkyne to allene and asymmetric synthesis of 2,5-dihydrofuran. J. Am. Chem. Soc 141, 3787–3791 (2019). [PubMed: 30789268]
20. See Supplementary Information Part 2 “Synthesis of Ligands and Catalysts” for details.
21. Schnabel C et al. Total synthesis of natural and non-natural Δ5,6Δ12,13-jatrophane diterpenes and their evaluation as MDR modulators. J. Org. Chem 76, 512–522 (2011). [PubMed: 21192665]
22. Dahlmann HA, McKinney AJ, Santos MP & Davis LO Organocatalyzed intramolecular carbonyl-ene reactions. Molecules 21, 713 (2016).
23. Amarasinghe KKD & Montgomery J. Enantioselective total synthesis of (+)-testudinariol a using a new nickel-catalyzed allenyl aldehyde cyclization. J. Am. Chem. Soc 124, 9366–9367 (2002). [PubMed: 12167019]
24. Zhou J, Yang M, Akdag A & Schneller SW C-4′ truncated carbocyclic formycin derivatives. Tetrahedron 62, 7009–7013 (2006).
25. Basak A, Chakrabarty K, Ghosh A & Das GK Theoretical study on the isomerization of propargyl derivative to conjugated diene under Au(I)-catalyzed reaction: A DFT study. Comput. Theor. Chem 1083, 38–45 (2016).
26. Xiao Y-C & Moberg C. Silaborative carbocyclizations of 1,7-enynes. Diastereoselective preparation of chromane derivatives. Org. Lett 18, 308–311 (2016). [PubMed: 26741486]
27. Fu J et al. Gold-catalyzed rearrangement of allylic oxonium ylides: efficient synthesis of highly functionalized dihydrofuran-3-ones. Angew. Chem., Int. Ed 52, 4198–4202 (2013).

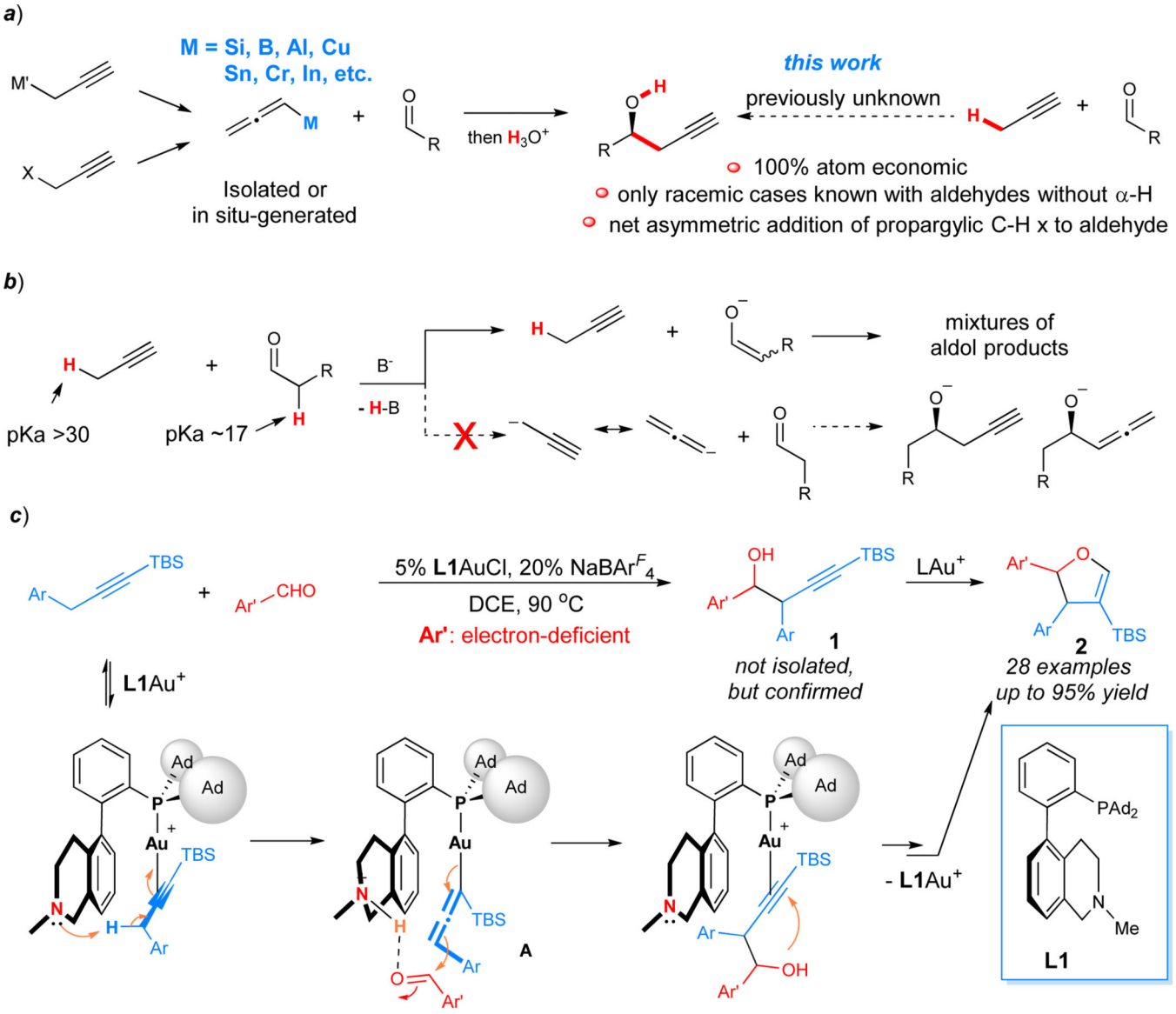

Fig. 1|. Asymmetric propargylation of aldehyde.

a) Strategies for asymmetric propargylation of aldehyde. **b**) Challenge in direct reacting propargylic C-H bond with aldehyde possessing α-hydrogens. **c**) Our previous work: intermolecular net racemic addition of propargylic C-H bond to aldehyde without α-C-H bond.

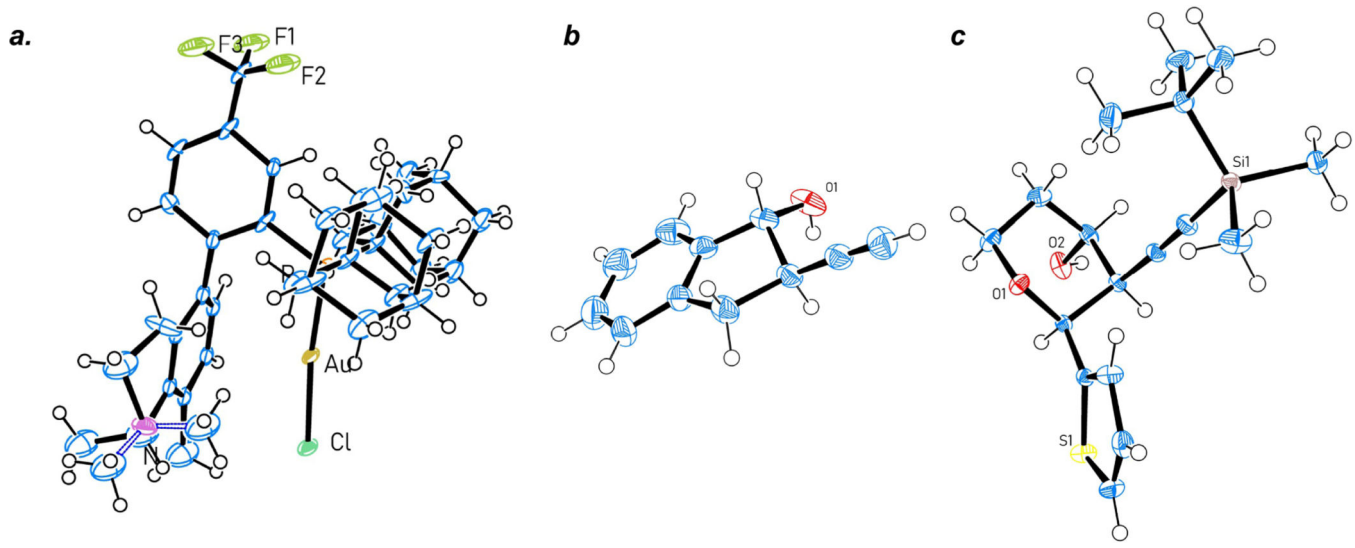

Fig 2|. ORTEP drawing of crystal structures (ellipsoid probability at 50%).
a) X-ray structure of (*S*)-**L3**AuCl (crystal CH_2Cl_2 omitted, and both *N*-methyl conformers detected). **b**) X-ray structure of **11**. **c**) X-ray structure of (*2S,3R,4S*)-**6p**.

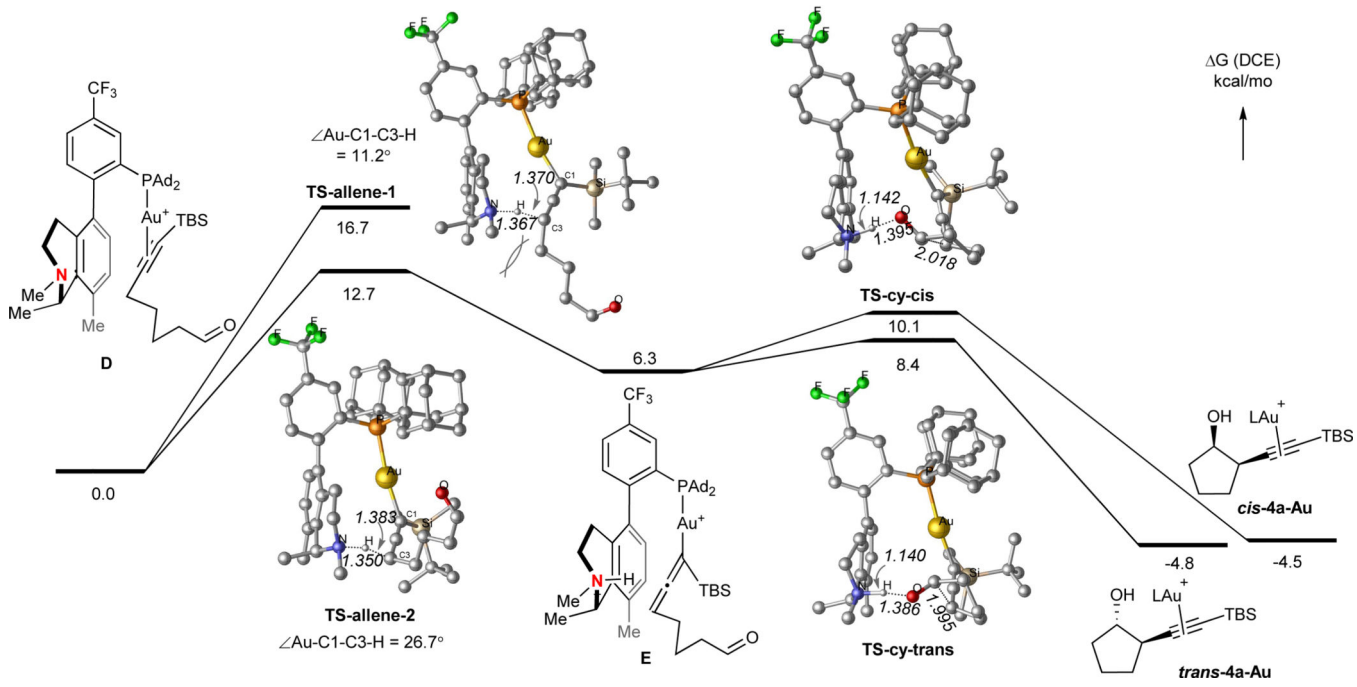

Fig. 3|. DFT-calculated energetics of the reaction of 3a in DCE.

Performed at PBE1PBE level using the effective core potential LANL2DZ for Au, the basis set 6–311g(d,p) for Si and P, and 6–31g(d,p) for the other atoms. The SMD model is employed for solvent DCE. The numbers in structures are in angstrom.

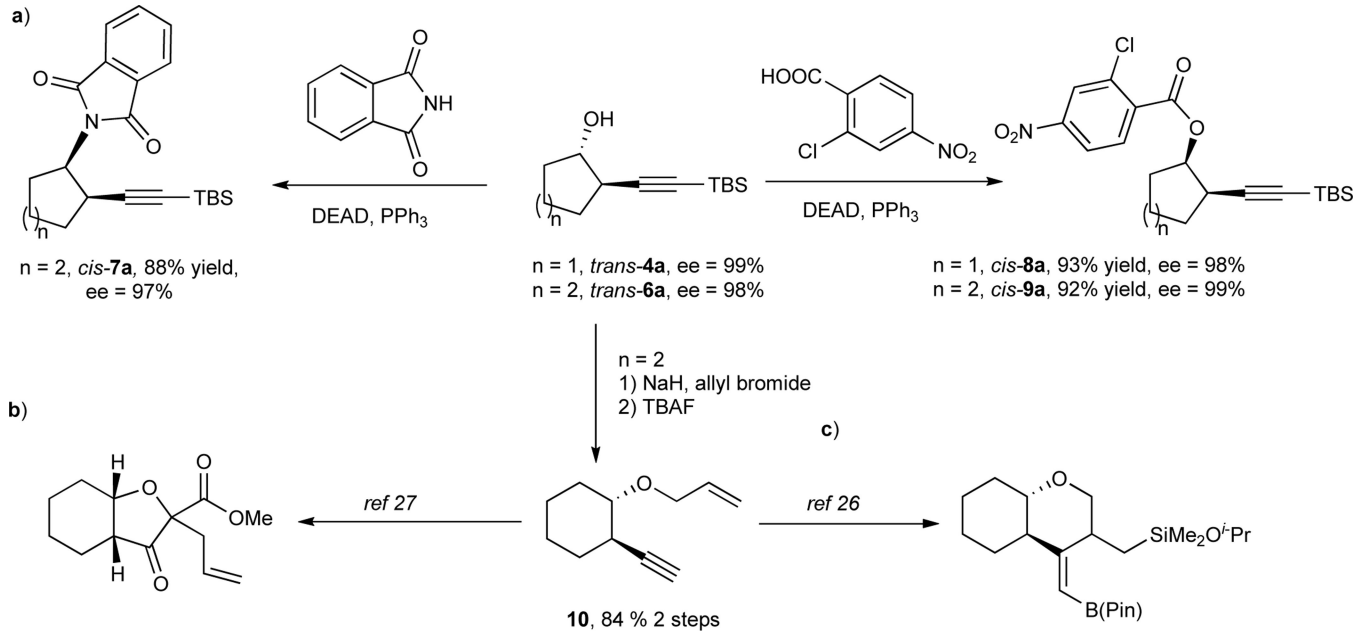

Fig 4|. Further transformations of the products.

a) the Mitsunobu reactions. **b**) An reported oxidative rearrangement**. c**) A reported silaborative cyclization.

Table 1.

Reaction discovery and Condition optimization.[a]

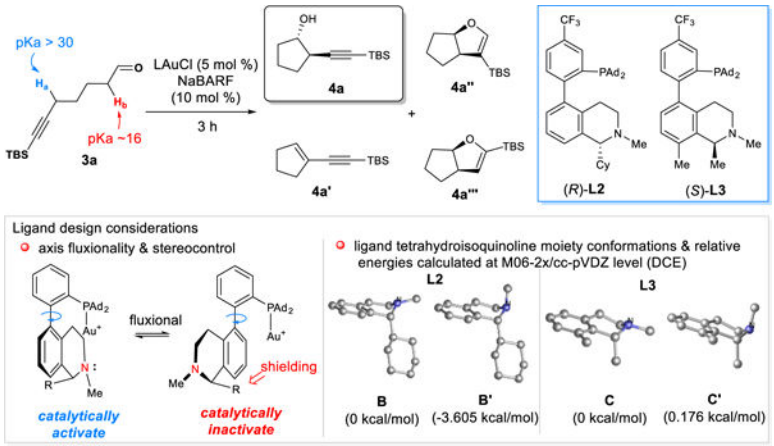

Entry	Ligand	Reaction conditions (3h)	Conver-sion (%)	Yield(%)[b] 4a/4a'/4a''/4a'''	ee (%)[c] (4a)
1	**L1**	NaBARF (10 mol %), DCE, 60°C	95	49/8/8/15	-
2	JohnPhos	NaBARF (10 mol %), DCE, 60°C	0	0	-
3	JohnPhos	NaBARF (10 mol %), DCE, 60°C, 10% Et_3N	0	0	-
4	(*R*)-L2	NaBARF (10 mol %), DCE, RT	70	55/−/−/−	−93
5	(*S*)-L3	NaBARF (10 mol %), DCE, RT	95	77/0/<3/<3	99
6	(*S*)-L3	AgOTf (10 mol %), DCE, RT	<10	0	-
7	(*S*)-L3	$AgNTf_2$ (10 mol %), DCE, RT	<10	0	-
8	(*S*)-L3	$Ag(CH_3CN)_2BArF_4$ (10 mol %), DCE, RT	60	40/−/−/−	99
9	(*S*)-L3	NaBARF (10 mol %), $PhCF_3$, RT	60	32/−/−/−	99
10	(*S*)-L3	NaBARF (10 mol %), THF, RT	57	33/−/−/−	99

[a] All reactions were run in sealed vials without replacing the atmosphere with Ar or N_2. DCE = 1,2-dichloroethane. THF = tetrahydrofuran. NaBARF = sodium tetrakis[3,5-bis(trifluoromethyl)phenyl]borate. Johnphos = (2-biphenyl)di-tert-butylph -osphine

[b] Isolated yields.

[c] Determined by HPLC using corresponding benzyl ester.

Table 2.

Scope toward the formation of five-membered ring-fused homopropargylic alcohols[a]

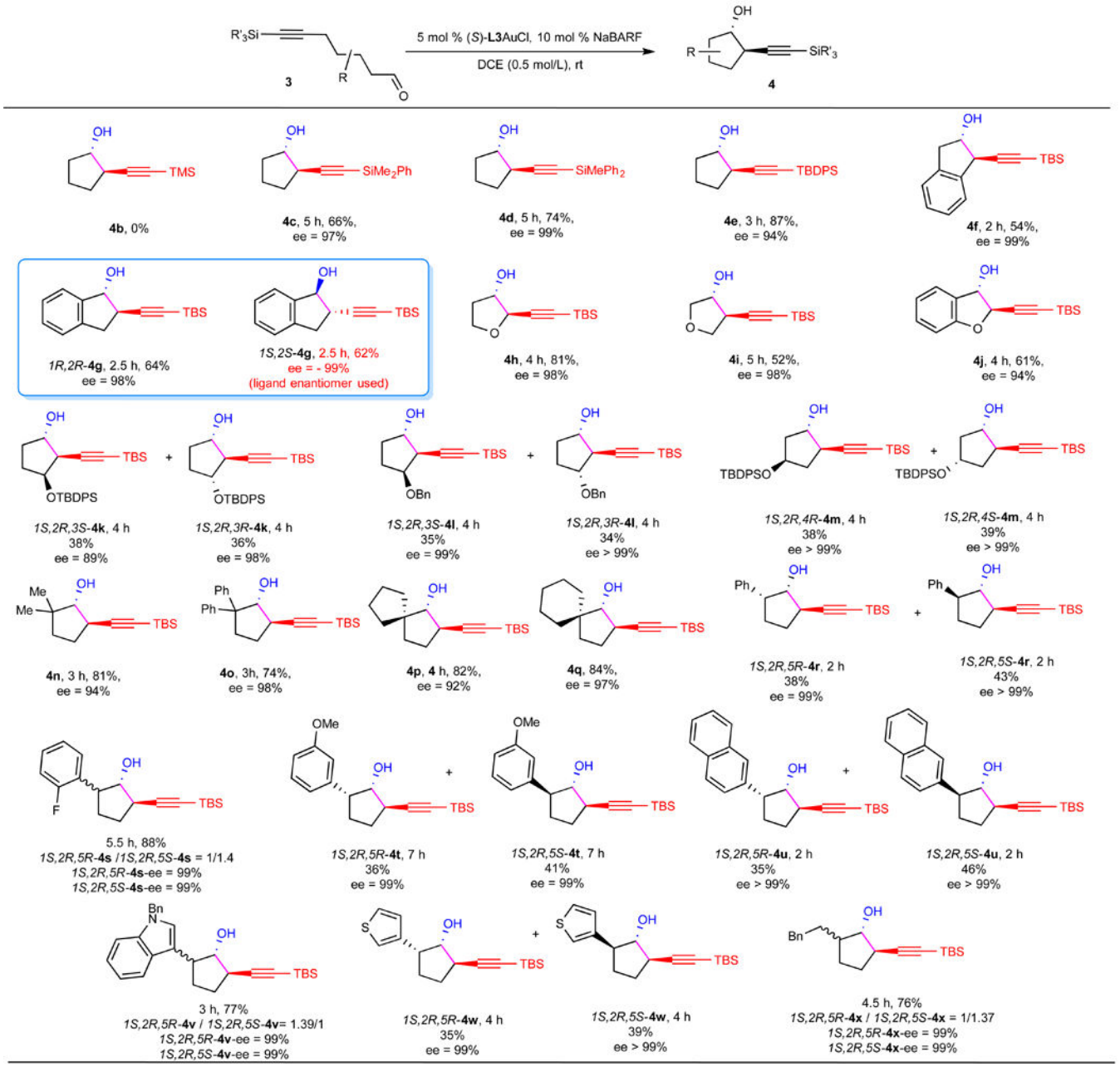

[a] All reactions were run in sealed vials with an initial substrate concentration of 0.5 M.

Table 3.

Reaction optimization for the formation of six-membered ring-fused homopropargylic alcohols[a]

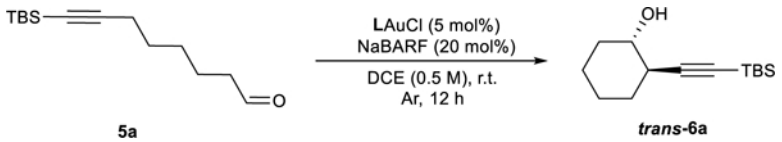

5a *trans*-6a

Entry	Ligand	Conversion	Yield (%)[c]	*ee* (%)[d]
1[b]	(*S*)-**L3**	<10	0	-
2	(*S*)-**L3**	95	70	98
3	(*R*)-**L2**	95	65	−76
4	(*R*)-**L3**	95	70	−99

[a]All reactions were run in sealed vials. DCE = 1,2-dichloroethane.

[b]Reaction was run under air condition, and 10 mol% $NaBAr^{F}_{4}$ was used.

[c]Isolated yields.

[d]Determined by HPLC using corresponding benzyl ester.

Table 4.

Scope toward the formation of six-membered ring-fused homopropargylic alcohols

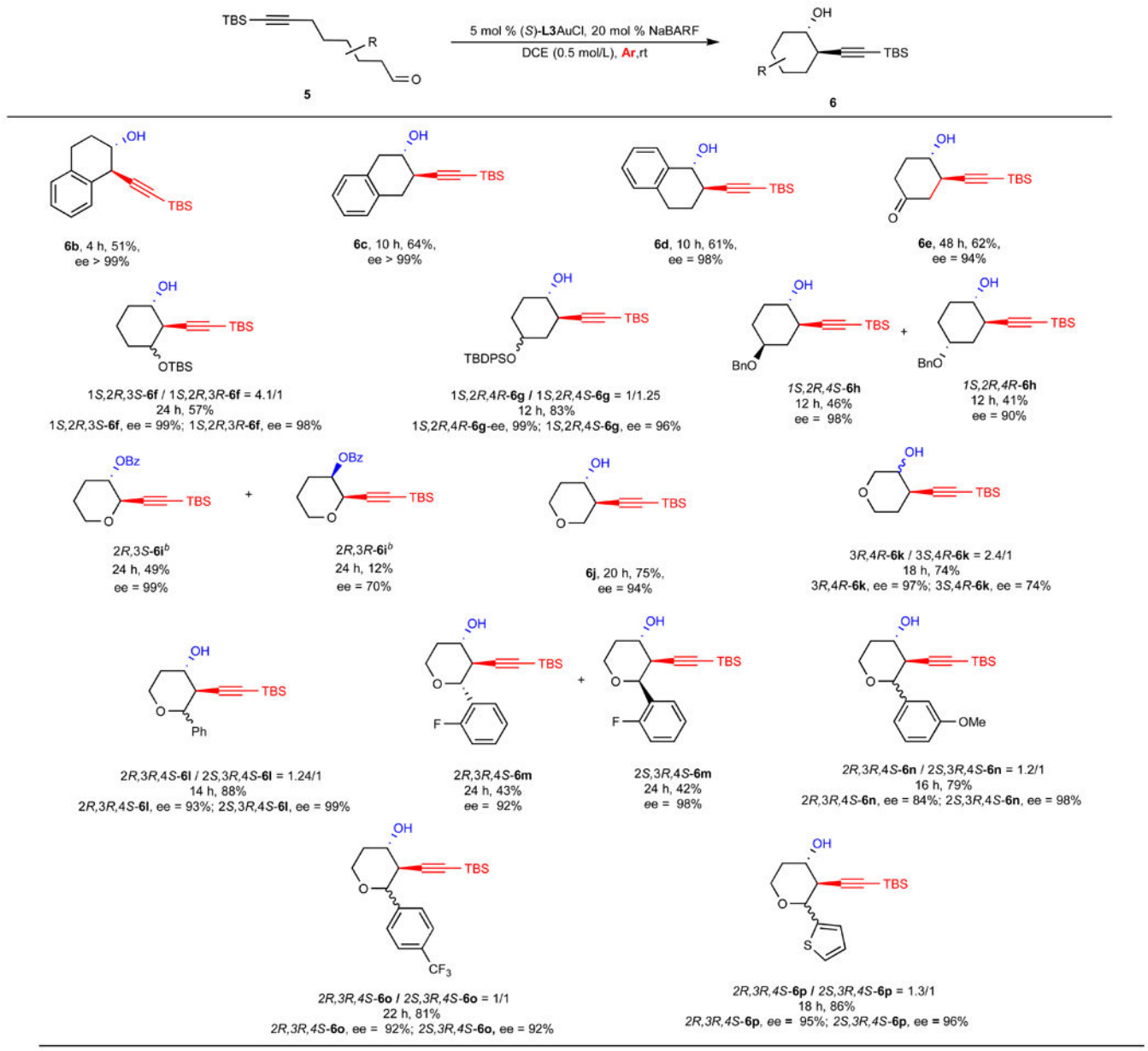

[a] All reactions were run in sealed vials with an initial substrate concentration of 0.5 M.

[b] The products are converted to benzoates and separated.